

CLMFormer: Mitigating Data Redundancy to Revitalize Transformer-based Long-Term Time Series Forecasting System

Mingjie Li, Rui Liu, Guangsi Shi, Mingfei Han, Changling Li, Lina Yao, *Senior Member, IEEE*, Xiaojun Chang, *Senior Member, IEEE*, and Ling Chen, *Senior Member, IEEE*

Abstract—Long-term time-series forecasting (LTSF) plays a crucial role in various practical applications. Transformer and its variants have become the de facto backbone for LTSF, offering exceptional capabilities in processing long sequence data. However, existing Transformer-based models, such as Fedformer and Informer, often achieve their best performances on validation sets after just a few epochs, indicating potential underutilization of the Transformer’s capacity. One of the reasons that contribute to this overfitting is data redundancy arising from the rolling forecasting settings in the data augmentation process, particularly evident in longer sequences with highly similar adjacent data. In this paper, we propose a novel approach to address this issue by employing curriculum learning and introducing a memory-driven decoder. Specifically, we progressively introduce Bernoulli noise to the training samples, which effectively breaks the high similarity between adjacent data points. To further enhance forecasting accuracy, we introduce a memory-driven decoder. This component enables the model to capture seasonal tendencies and dependencies in the time-series data and leverages temporal relationships to facilitate the forecasting process. The experimental results on six real-life LTSF benchmarks demonstrate that our approach can be seamlessly plugged into varying Transformer-based models, with our approach enhancing the LTSF performances of various Transformer-based models by maximally 30%.

Index Terms—Long-term time series forecasting, Transformer, Curriculum learning, Memory module

I. INTRODUCTION

LONG-TERM time series forecasting (LTSF) stands as a cornerstone within a multitude of practical applications for complex real-life scenarios, such as finance [1], traffic, weather [2] and hospital admission rates prediction [3], wielding the power to shape crucial outcomes. Witness the success of Transformer [4] and further applications in numerous fields [5]–[11], researchers have begun to utilize the Transformer and its evolutionary descendants [12]–[15] as the de facto backbone in this intricate landscape. It showcases unparalleled prowess in handling extensive sequence data, elucidates patterns, and unveils latent structures that under-

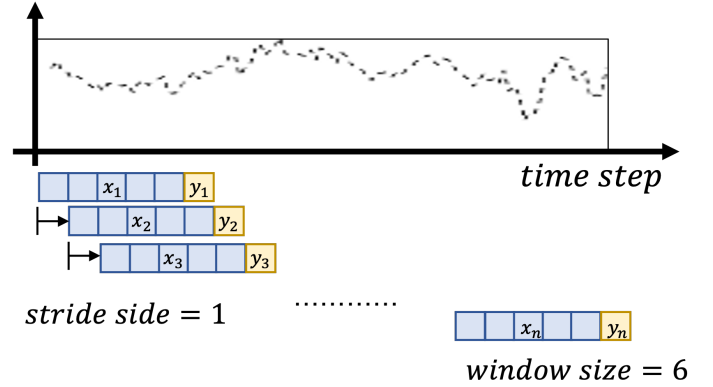


Fig. 1: Illustration of the rolling forecasting setting with stride size=1.

score sequential phenomena. More details, these Transformer-based LTSF systems have demonstrated strong performance, for which they can predict hundreds of time steps ahead, in contrast to other sequence processing networks and traditional methods that were mostly only capable of making predictions for 48-time points or less [16]–[18]. The spotlight on the Transformer architecture within LTSF illuminates a sophisticated symphony of computation, where self-attention mechanisms and hierarchical processing harmoniously intertwine. This orchestration empowers these models to decipher intricate temporal intricacies and discern long-range dependencies embedded within extensive sequences [19].

Strikingly, when playing with these Transformer-based LTSF systems [4], [14], [15], [19], we observed that these models frequently attain their apex performance on validation datasets within a remarkably abbreviated span of training epochs, sometimes even the first epoch [15], and then the performances dropped gradually. This observation hints at the latent underexploitation of the Transformer-based systems’ innate potential. The emergence of such a phenomenon can typically be attributed to a confluence of two primary factors: insufficient training data and the constrained parameter within the network architecture. However, the inherent modularity of these architectures allows for facile parameter augmentation by virtue of stacking additional Transformer modules. This architectural extensibility, coupled with the recognition that the constrained parameter space might not be the predominant

Manuscript submitted Feb 2024.

M. Li is with the Radiation Oncology, at Stanford University. This work was done when M. Li was with the University of Technology Sydney. The code is available at github.com/mlii0117/CLMFormer.

R. Liu, M. Han, C. Li, X. Chang and L. Chen are with The ReLER Lab, Australian Artificial Intelligence Institute, Faculty of Engineering and Information Technology, University of Technology Sydney, Australia.

G. Shi is with the Faculty of Information Technology, Monash University. M. Han and L. Yao are with the CSIRO’s Data61, Australia.

bottleneck, guides our inference toward the more probable origin: the paucity of comprehensive and high-quality training data.

Delving further into this phenomenon, we found that there is severe data redundancy within the training samples, stemming from the common practice of rolling forecasting settings (see Figure. 1 for more details) during data augmentation. Under the rolling forecasting setting, if the stride size is 1, then the previous and current training samples are only one data point apart from each other. Since making longer predictions typically requires longer input sequences, training samples for LTSF models have a higher degree of similarity. For example, when the model’s input length is 2, the similarity between two consecutive training inputs is 50% (1/2); however, if we increase the model’s input length to 168, the similarity between two consecutive training inputs rises to 99.4% (167/168). Therefore, the LTSF models are more likely to suffer from overfitting due to such data redundancy. One could argue that we could decrease the training sample similarities by increasing the stride size; however, the number of training samples decreases by the factor of the stride size, as the training sample numbers are calculated by:

$$N_t = \frac{N_d - S_w + 1}{S_s}. \quad (1)$$

where N_t represents the number of training samples, N_d represents the total number of time points in the training data, S_w refers to the window size, and S_s is the stride size. Although increasing stride sizes can decrease the sample similarities, it causes a decrease in training sample numbers, which also increases the likelihood of overfitting.

To address the aforementioned data redundancy issue, we propose CLMFormer, a novel pipeline with curriculum learning and a memory-driven decoder, designed to revitalize varying Transformer-based LTSF systems. Since data redundancy directly results from the heightened similarity present within the training data, our priority is to break this similarity while concurrently preserving the necessary training sample volume. To achieve this, we leverage the concept of curriculum learning [20]–[22], gradually increasing training difficulty and data variety by progressively introducing Bernoulli noise to the training data through a dynamic dropout scheme. Such a scheme reduces the propensity for overfitting while simultaneously enhancing the model’s capacity to capture sequential patterns. To further enhance the Transformer’s ability to recognize intricate sequential patterns from highly similar training data, we propose a memory-driven decoder to facilitate the forecasting process. This is accomplished by adopting a seasonal memory and memory-conditioned layer normalization operation, both of which effectively utilize past time-series information and introduce additional computations to enhance the model’s capability for complex pattern recognition. The main contributions of this paper are summarized as follows:

- We uncover the swift validation peak in Transformer-based LTSF systems, attributed to data redundancy stemming from rolling forecasting settings.
- We propose a novel pipeline, CLMFormer, introducing curriculum learning and a memory-driven decoder to revitalize Transformer-based LTSF systems.
- We employ a progressive training schedule to increase the training difficulty and data variety and propose a seasonal memory matrix to recognize sequential patterns from highly similar training data.
- Extensive experiments are performed, and the results show that our method can be seamlessly plugged into various transformer-based LTSF models and improve their performances by maximally 30%.

II. RELATED WORK

A. Time Series Forecasting

Time series forecasting (TSF) [23] is a critical task in various domains, encompassing domains such as finance, energy, healthcare, and more. Early approaches to TSF often revolved around traditional statistical and machine learning methods. These methods include ARIMA models [24], exponential smoothing methods [25], and seasonal decomposition of time series algorithms [26]. These techniques have been widely used due to their simplicity and interpretability. However, they often struggle to capture intricate temporal patterns and dependencies present in real-world data.

In recent years, deep learning techniques have gained traction for TSF. RNNs, including LSTM [16], GRU [27] and DeepAR [28], have demonstrated their capability to capture temporal patterns. However, these models easily suffer from error accumulation, a phenomenon where small errors generated during earlier time steps can propagate and magnify as the sequence progresses [29]. This issue can significantly impact the overall accuracy and stability of the model’s predictions, especially in long sequences or when dealing with complex relationships within the data.

B. Transformer-based LTSF Systems

Due to the superior performances in processing sequence data, Transformer-based models have achieved state-of-the-art results in many time-series tasks [30], especially in LTSF problems [12], [15], [19], [31]. There are several areas of focus among the latter studies. Some have focused on reducing the computational costs to enable longer predictions by sparse attention, whereby the memory cost is reduced from $O(L^2)$ to as low as $O(L \log L)$ [15], [32], where L refers to the sequence length in attention layers. Other studies aim at improving the architecture or patch representations to further enhance the Transformer’s ability to learn seasonal and intricate temporal patterns. The Autoformer model [19] introduces an innovative Auto-Correlation mechanism that enables sub-series level aggregation, effectively addressing the inherent periodicity within time series data. FEDformer [14], on the other hand, focuses on learning a sparse temporal representation through the utilization of frequency-enhanced blocks/attention. This approach involves leveraging a random subset of frequency components along with learnable complex-number parameters. Another recent development, InParformer [12], incorporates evolutionary seasonal-trend decomposition modules and an

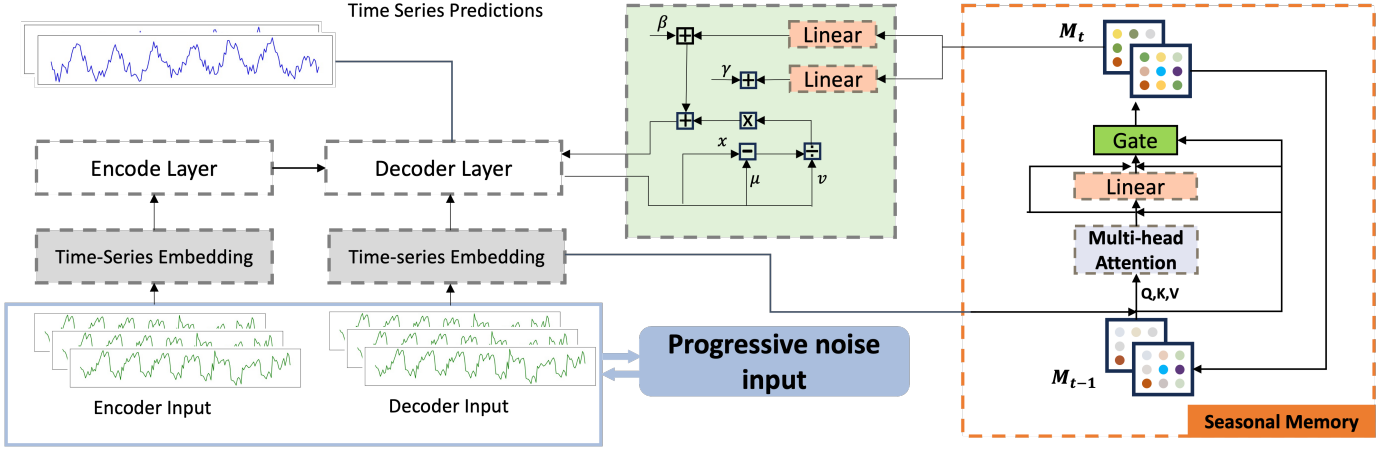


Fig. 2: An overview of the model architecture. M_{t-1} represents the memory matrix from the previous prediction, M_t represents the updated memory matrix during the current sequence prediction, which in turn is recycled to be the M_{t-1} for the next prediction.

interactive parallel attention mechanism with frequency-aware attention and time-aware attention, enhancing its ability to capture meaningful patterns within time series data. PatchTST [13] adopts subseries-level patches and channel independence to improve the capability of representation learning. Despite the significant progress made, Zeng et al. [33] argued that Transformer-based LSTF models are underutilized. They proposed a simple linear model that achieved superior performance. In this paper, we revisit these models and uncover the issue attributed to data redundancy stemming from rolling forecasting settings.

III. APPROACH

In this section, we present our solutions to revitalize Transformer-based systems that specifically target the challenges for LSTF. Our approach is based upon the Transformer architecture; we aim to enhance Transformer models on LSTF problems by making improvements to mitigate data redundancy from both training optimization prospects and the architecture. The overview of our approach is illustrated in Figure. 2. Our model comprises three major elements, namely the input embedding, the main Transformer-based model, and the seasonal memory component, whereby we propose to train the model based on a progressive training strategy. We first introduce the background of employing Transformer models for LSTF and then describe the training strategy. The seasonal memory component is described in the remaining subsections.

Typical Transformer-based LSTF models normally train under rolling forecasting settings with a fixed window and a stride size = 1, as shown in Figure 1. The input data at time t can be written as $X^t = \{x_1^t, x_2^t, \dots, x_{L_S}^t | x_k^t \in \mathbb{R}^{d_f}\}$, where L_S is the input length and the feature dimension $d_f > 1$. Moreover, the model output is $Y^t = \{y_1^t, y_2^t, \dots, y_{L_p}^t\}$, where L_p is the prediction length, and the output feature dimension is flexible and is not limited to single sequence predictions.

A. Base Model

1) *Input Embedding*: The input data are first passed through an embedding. Different from other types of sequential data, in time series problems, the model should capture the time information. This is extremely crucial in LSTF settings, as models are required to make predictions up to weeks in advance. We decided to utilize the time-series-specific embedding method proposed by [15]. The method applies a combination of the context vector, the positional embedding, and the seasonal embedding. The context vector $u^t \in \mathbb{R}^{L_S * d_{model}}$ is obtained by projecting the model input $X^t \in \mathbb{R}^{L_S * d_f}$ into a dimension of d_{model} by an 1-D convolutional layer. The goal of the context vector is to transform the input data into an appropriate dimension. The positional embedding (PE(pos)) and the seasonal embedding (SE(pos)) are used to capture the local context and the global time feature, respectively. The formula for the input embedding is:

$$X_{embed}^t = \delta u^t + \text{PE}(\text{pos}) + \sum_k [\text{SE}(\text{pos})]_k \quad (2)$$

Where $X_{embed}^t \in \mathbb{R}^{L_S * d_{model}}$ is the embedded model input, δ is the weight factor to balance between the embeddings and the context vector and k represents the levels of the seasonal components, *i.e.* days, weeks, seasons, holidays.

2) *Encoder-Decoder Architecture*: The backbone of our method lies in Transformer-based models following an encoder-decoder structure. Despite some minor differences between different variants, their general purpose is the same. The encoder takes past input sequences into the model and generates hidden states as outputs that contain time pattern information, which the decoder uses to make predictions. We decided to use generative-style decoding [15], which has been proven to achieve superior performances in LSTF problems and have exponentially better computational efficiency than conventional dynamic decoding [34]. The generative-style decoding generates all predictions in one step, with the decoder feeding vector $X_{feed,dec}^t$ presented as:

$$X_{feed,dec}^t = \text{Concat}(X_{dec}^t, X_0^t) \in R^{(L_{dec}+L_p)*d_f}, \quad (3)$$

where $X_{dec}^t \in R^{L_{dec}*d_f}$ is the time-series input sequence for the decoder, L_{dec} is the length of the decoder time-series input, $X_0^t \in R^{L_p*d_f}$ is the placeholder for the prediction sequence, and the L_p is the prediction length.

3) *Loss Function*: The loss function we use is Mean Squared Error (MSE) loss on the target sequences, and it is then backpropagated across the entire network.

$$L_{MSE} = \frac{1}{n} \sum_{i=1}^n (y_i - \hat{y}_i)^2 \quad (4)$$

where y_i is the true value for the i^{th} time step in the output sequence, \hat{y}_i is the predicted value, and n is the total number of values. Both y_i and \hat{y}_i have a dimension of ≥ 1 .

B. Progressive Training Strategy

As mentioned before, we argued that the under-exploitation of Transformer-based LTSF models attributed to the heightened similarity within the training samples stemming from rolling forecasting settings. Therefore, we decided to break these similarities during the training process but kept the rolling forecasting settings. Because it does augment the training samples effectively and efficiently. Since increasing stride size for the rolling window does not help with the overfitting issue, inspired by the masking strategy [34], we decided to mitigate the data redundancy issue by adding sample variety. These noises should be added in a manner such that the rate is slower at the beginning to ensure that the model has a good grasp of the data pattern before we start to increase the rate of introducing noises to prevent the model from overfitting. To achieve this goal, we decided to alter dropout rates, as there is a proven connection between dropout and noises [35]–[37]. We dynamically alter the dropout rate during training based on a monotone function proposed by [38], whereby the function rate starts slower and later increases as training proceeds. The dropout rate function is based on:

$$\theta_d(t) = \min(\theta_{max}, 1 - \theta_{max} - (1 - \theta_{max}) \exp(-\gamma t)) \quad (5)$$

where t is the t^{th} number of 100 iterations, θ_d is the dropout rate, θ_{max} is the maximum dropout rate, and γ is a hyperparameter typically set between 0.001 to 0.01.

C. Seasonal Memory-driven Forecasting

After adding noise to increase the data variety, it is critical to improve the models' capability to capture long dependencies and intricate temporal patterns. In this paper, we introduce a seasonal memory-driven decoder to facilitate the forecasting process. Applications of the memory concept have demonstrated superior performances in a variety of sequential tasks [39]–[41]. In particular, [42] demonstrated that the memory concept is effective in improving LSTM's ability on multivariate TSF. Therefore, we argued that this concept should also work on Transformer models under the multivariate forecasting setting.

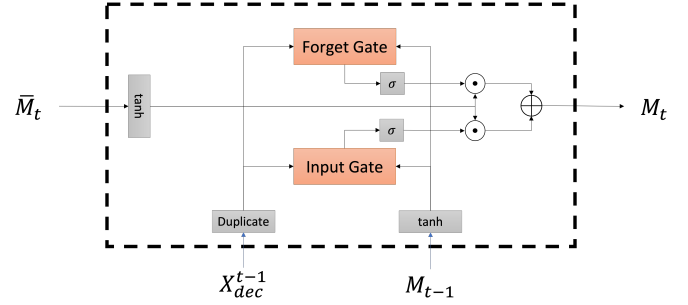


Fig. 3: Overview of the gate mechanism.

There are various ways of implementing memory into Transformers [43]–[47]. Our goal is to enhance the Transformer's ability on both handling increased data complexity brought and recognizing hidden sequential patterns from highly similar training data. We decided to incorporate a memory unit into the decoder block because the decoder block is highly relevant to the output predictions. To achieve this goal, we proposed a seasonal memory, having a self-attention layer that can help to further analyze the hidden sequential patterns that are missed by the encoder-decoder component by combining information stored in the memory matrix together with the model input. The way to connect the seasonal memory block to the decoder is via a memory-driven conditional layer normalization (MDCLN) layer, the general formula for this connection can be written as:

$$\text{MDCLN}(\text{Att}(h_{l-1}), M_t) \quad (6)$$

where MDCLN(.) is the memory-driven conditional layer normalization, Att(.) represents the attention layer in the decoder block, h represents the output state from the previous layer $l - 1$, and M_t refers to the updated memory matrix at time point t .

1) *Memory-driven Conditional Layer Normalization*: The Memory-driven Conditional Layer Normalization (MDCLN) is a way to integrate seasonal memory into the decoder, where outputs from the decoder's self-attention layer undergo layer normalization along with the memory information provided from the seasonal memory block. The reason for using layer normalization instead of batch normalization is that input data are normalized before feeding into models as common practice for time-series forecasting. Hence, instead of normalizing values among batches, we use layer normalization to normalize the features within each batch to give each time feature an equal weight for generating predictions.

In MDCLN, we update γ and β based on the memory matrix M_t , as they are the two most essential parameters for normalization:

$$\gamma_t = \gamma + f_l(M_t), \quad (7)$$

$$\beta_t = \beta + f_l(M_t). \quad (8)$$

Where $f_l(\cdot)$ represents the linear layer. The MDCLN is achieved by:

$$\text{MDCLN}(h_{l-1}, M_t) = \gamma_t \odot \frac{h_{l-1} - \mu}{\sigma} + \beta_t + f_t. \quad (9)$$

Where μ and σ are the mean and standard deviation of h_{l-1} , and h_{l-1} is the output of self-attention at layer $l - 1$ in the decoder.

2) *Seasonal Memory Matrix*: In addition to the further calculations that the seasonal memory unit can bring, another main characteristic of this unit is that it can read/write information from/to a memory matrix which assists with analyzing time patterns. In NLP problems, we use dynamic decoding [34]; the memory matrix works by maintaining information from the prediction of the last token/word while predicting a paragraph, and this matrix is re-initialized after each paragraph, as each paragraph is perceived as being independent. However, as explained above, we use generative-style decoding for our task, in which it generates all predictions in a single step [15]. In this case, the traditional matrix initialization method will not work, as we do not generate individual time point predictions one by one. In addition, for each forecasting problem, the input sequences for making previous predictions are still helpful for any future prediction, as they come from the same time series and share similar pattern interactions. Therefore, we maintain a memory matrix for each specific forecasting task, where we keep the matrix output from the seasonal memory at the prediction time point $t - 1$ as the input matrix at time point t ; this matrix is updated after every prediction by a gating mechanism to control the ratio of the memory matrix being updated. Since more recent model inputs are weighted higher than those from the distant past, the matrix can maintain all relevant time information. In addition, this matrix will continue updating even after training, which ultimately increases the model’s generalization power. The seasonal memory unit updates the memory matrix by first calculating the self-attention based on the matrix M at time point $t - 1$, where $Q = M_{t-1} \times W_q$, $K = [M_{t-1}; \text{embed}(X_{feed,dec}^t)] \times W_k$ and $V = [M_{t-1}; \text{embed}(X_{feed,dec}^t)] \times W_v$. The W_k , W_v and W_q are trainable weights, and $[M_{t-1}; \text{embed}(X_{feed,dec}^t)]$ is the row-wise concatenations between M_{t-1} and the embedded decoder feeding vector. We then calculate the self-attention score Z from Q , K and V . After the self-attention layer, we go through a feedforward layer to produce \bar{M}_t , which is calculated as:

$$\bar{M}_t = \text{Feedforward}(Z + M_{t-1}) + Z + M_{t-1} \quad (10)$$

\bar{M}_t is then passed through a gating mechanism to calculate the ratio of the \bar{M}_t to be added to the final M_t :

$$M_t = \sigma(G_f^t) \odot M_{t-1} + \sigma(G_i^t) \odot \bar{M}_t, \quad (11)$$

where G_i^t is the input gate, G_f^t is the forget gate, \odot is the Schur product, and $\sigma(\cdot)$ is the sigmoid function.

3) *Gate Mechanism*: The gate mechanism decides the proportion of new information from \bar{M}_t to incorporate and the proportion of M_{t-1} to discard to produce the final M_t . As shown in Figure. 3, the gate mechanism has two key components: the input gate G_i^t and the forget gate G_f^t . The

two gates are calculated by balancing the embedded decoder input $X_{feed,dec}^{t-1}$ and the previous memory matrix at $t - 1$ (M_{t-1}), where we duplicate the $\text{embed}(X_{feed,dec}^{t-1})$ to match the dimension of M_{t-1} . These two gates have the following formulas:

$$G_i^t = \text{embed}(X_{feed,dec}^{t-1}) \times W_i + \tanh(M_{t-1}) \times U_i, \quad (12)$$

$$G_f^t = \text{embed}(X_{feed,dec}^{t-1}) \times W_f + \tanh(M_{t-1}) \times U_f. \quad (13)$$

Where W_i , W_f , U_i , and U_f are trainable weights for the two gates.

IV. EXPERIMENTS

A. Datasets

We conduct extensive experiments on 6 public real-life benchmark datasets. For all datasets, train/valid/test sets are split follow the ratio of 0.7/0.1/0.2 in chronological order. **ETT** (Electricity Transformer Temperature) [15]. The dataset contains information about six power load features and the target value “oil temperature”. We use the two hourly datasets from the source named as Etth_1 and Etth_2 . We use the first 20 months of data; **Weather**¹. The dataset contains hourly data about climate information from around 1,600 locations in USA between 2018 and 2020. The data consist of seven quantitative climatological features with “dry bulb temperature” as the target; **Air Quality**². The dataset consists of eleven quantitative hourly features relevant to air quality with the target value set as “PM10” from 12 national air quality monitoring sites. We use the data from the “Wanshouxigong” station; **Traffic**³. The dataset contains the traffic condition data measured in the of between Minneapolis and St Paul, Minnesota, USA. The dataset has five hourly numerical features with the target value of “traffic volume”. **Exchange**⁴. The collection of the daily exchange rates of eight foreign countries including Australia, British, Canada, Switzerland, China, Japan, New Zealand and Singapore ranging from 1990 to 2016.

B. Experimental Details

1) *Baselines*: We use four Transformer variants as our baseline with generative-style decoding to generate the output sequences in one step [15]. These models are FEDformer [14], AutoFormer [19], Informer [15] and the vanilla Transformer [4], respectively. In addition, since traditional methods like ARIMA and RNNs-based networks lack competitive performance [12], [14], we only compared our model’s performances with the SOTA Transformer-based model, InParformer [12].

¹<https://www.ncei.noaa.gov/data/local-climatological-data>

²<https://archive.ics.uci.edu/ml/datasets/Beijing+Multi-Site+Air-Quality+Data>

³<https://archive.ics.uci.edu/ml/datasets/Metro+Interstate+Traffic+Volume>

⁴https://github.com/laiguokun/multivariate-time-series-data/blob/master/exchange_rate

TABLE I: The multivariate results comparison of our method with the SOTA Transformer-based LTSF models (three repetitions). The numbers in bold indicate the better-performing models within each Transformer-based LTSF model pair.

Methods		FedFormer+ours		FedFormer		Informer+ours		Informer		Transformer+ours		Transformer	
Metric		MSE	MAE	MSE	MAE	MSE	MAE	MSE	MAE	MSE	MAE	MSE	MAE
Eth1	24	0.304	0.370	0.315	0.381	0.495	0.493	0.550	0.541	0.474	0.493	0.456	0.474
	48	0.335	0.381	0.338	0.392	0.582	0.555	0.644	0.606	0.585	0.568	0.608	0.584
	168	0.407	0.438	0.420	0.443	0.981	0.771	1.110	0.861	0.914	0.750	0.925	0.767
	336	0.451	0.454	0.459	0.465	1.098	0.816	1.237	0.893	1.001	0.801	1.077	0.821
	720	0.467	0.489	0.506	0.507	1.156	0.842	1.475	0.993	1.164	0.871	1.182	0.872
Eth2	24	0.224	0.316	0.220	0.312	0.542	0.560	0.385	0.467	0.534	0.581	0.474	0.522
	48	0.271	0.358	0.284	0.47	1.190	0.873	1.959	1.119	0.909	0.761	1.063	0.832
	168	0.405	0.410	0.412	0.427	4.869	1.856	5.957	2.036	4.951	1.807	4.067	1.623
	336	0.481	0.469	0.496	0.487	4.672	1.872	4.303	1.780	4.371	1.727	3.852	1.613
	720	0.442	0.453	0.463	0.474	3.358	1.569	3.444	1.574	3.690	1.671	2.603	1.369
Air	24	0.590	0.411	0.588	0.412	0.542	0.374	0.562	0.388	0.560	0.383	0.552	0.380
	48	0.694	0.459	0.686	0.457	0.650	0.435	0.692	0.447	0.679	0.440	0.698	0.448
	168	0.805	0.504	0.816	0.515	0.720	0.479	0.883	0.518	0.780	0.502	0.798	0.499
	336	0.827	0.515	0.834	0.518	0.773	0.505	0.852	0.536	0.789	0.501	0.823	0.514
	720	0.885	0.526	0.898	0.540	0.793	0.503	0.861	0.534	0.840	0.514	0.859	0.524
Traffic	24	0.611	0.412	0.556	0.364	0.324	0.222	0.381	0.264	0.337	0.248	0.411	0.282
	48	0.588	0.373	0.561	0.359	0.351	0.243	0.440	0.300	0.364	0.275	0.486	0.336
	168	0.587	0.364	0.612	0.381	0.405	0.300	0.567	0.396	0.407	0.300	0.555	0.384
	336	0.584	0.350	0.621	0.383	0.397	0.291	0.572	0.399	0.413	0.302	0.570	0.400
	720	0.597	0.351	0.626	0.382	0.468	0.330	0.585	0.400	0.392	0.293	0.585	0.399
Weather	24	0.148	0.231	0.162	0.247	0.253	0.338	0.258	0.342	0.253	0.340	0.263	0.352
	48	0.189	0.274	0.204	0.293	0.344	0.411	0.354	0.418	0.338	0.414	0.348	0.419
	168	0.263	0.325	0.284	0.347	0.507	0.520	0.578	0.544	0.513	0.512	0.551	0.526
	336	0.305	0.356	0.349	0.390	0.545	0.537	0.591	0.553	0.512	0.507	0.584	0.547
	720	0.384	0.395	0.413	0.428	0.593	0.567	0.625	0.643	0.554	0.530	0.642	0.576

TABLE II: Key parameters for backbones.

Prediction Len.	{24,48}	{168,336}	{720}
d_{model}	1024	1024	1024
d_{ff}	2048	2048	2048
n_heads	8	8	8
Dropout	0.1	0.1	0.1
Activation	GELU	GELU	GELU
Batch Size	32	8	4
Enc.Layer no.	1	2	2
Dec.Layer no.	1	1	1

TABLE III: Key parameters for the seasonal memory unit.

	AutoFormer	Fedformer	Informer
d_{rm}	1024	1024	1024
Mem.slot.no.	1	1	1
Mem.head.no.	2	2	4

2) *Implementation Details*: Our model is constructed based on Pytorch with Python 3.7. We use a single NVIDIA GeForce RTX 3080Ti GPU for training. All of the input data undergo normalization before being fed into the model. The training is performed under the rolling forecasting setting (stride size=1). The encoder and decoder input lengths are {48, 96, 168, 168, 336} and {48, 48, 168, 168, 336}, which correspond to the prediction lengths of {24, 48, 168, 336, 720}, respectively. For the progressive training scheme, we update the dropout rate for every 100 iterations with the upper dropout limit of 0.1. Moreover, we apply an early stopping technique with patience=3 during training and the training epoch is set to be 10. The learning rate starts from 0.0001 and it halves its

value for every epoch after the first two epochs.

3) *Model Reproducibility*: To ensure model reproducibility, we present detailed parameter settings in this section. Table II describes the details for all Transformer-based models. We use the same setting for all three Transformer-based models in our experiment because these three models share a very similar structure and show optimal performance under similar settings. However, we use different settings for different prediction output lengths to adjust the model for different prediction tasks. Table II specifies the model dimension (d_{model}), the dimension of positional feedforward layers inside the encoder and decoder block (d_{ff}), and the number of attention heads in each attention layer (n_heads). In addition, we include information about batch size, layer activation function, the encoder layer number (Enc.Layer no.), and the decoder layer number (Dec.Layer no.). Table III describes the parameters for the relational memory block. There are three key parameters for the relational memory unit: the unit dimension (d_{rm}), the number of memory units (Mem.slot.no), and the number of attention heads in the relational memory (Mem.head.no). Here, we apply different relational memory settings for the three Transformer-based models as they require different settings to achieve optimal performance.

We use two evaluation metrics to measure our model performance: Mean Squared Error (MSE) and Mean Absolute Error (MAE).

C. Multivariate Results

Table I summarizes the multivariate results of the Transformer-based LTSF models and our proposed methods.

TABLE IV: The univariate results comparison of our method with the Transformer-based LTSF models. The numbers in bold and red indicate the better-performing models within each Transformer-based LTSF model pair and comparing to the InParformer.

Methods		FedFormer+ours		FedFormer		AutoFormer+ours		AutoFormer		InParformer	
Metric		MSE	MAE	MSE	MAE	MSE	MAE	MSE	MAE	MSE	MAE
Weather	96	0.0065	0.062	0.0062	0.062	0.0111	0.083	0.0110	0.081	0.0022	0.036
	192	0.0061	0.062	0.0060	0.062	0.0074	0.067	0.0075	0.067	0.0038	0.048
	336	0.0039	0.048	0.0041	0.050	0.0060	0.059	0.0063	0.062	0.0033	0.045
	720	0.0051	0.058	0.0055	0.059	0.0079	0.066	0.0085	0.070	0.0030	0.042
ETTh2	96	0.126	0.270	0.128	0.271	0.150	0.301	0.153	0.306	0.117	0.264
	193	0.188	0.319	0.185	0.330	0.200	0.347	0.204	0.351	0.169	0.319
	336	0.221	0.364	0.231	0.378	0.238	0.382	0.246	0.389	0.225	0.373
	720	0.267	0.406	0.278	0.420	0.252	0.398	0.268	0.409	0.241	0.399
Exchange	96	0.155	0.301	0.154	0.304	0.239	0.388	0.241	0.387	0.105	0.247
	193	0.284	0.427	0.286	0.420	0.295	0.366	0.300	0.369	0.207	0.360
	336	0.498	0.552	0.511	0.555	0.498	0.517	0.509	0.524	0.400	0.498
	720	1.126	0.860	1.301	0.879	1.167	0.832	1.260	0.867	1.172	0.836

We applied the same setting for each transformer-based model pair to achieve a fair comparison. Based on the results in Table I, we find that: (1) Our model can significantly improve the Transformer-based LTSF models’ performances up to 30% on multivariate LTSF problems across most cases; it improves the MSE and MAE scores in 20 of 25 prediction tasks in FEDformer, 23 of 25 prediction tasks in Informer and 19 of 25 tasks in vanilla Transformer. Our results show that our proposed CLMFormer with the progressive training schedule and memory-driven decoder can help Transformers with multivariate LTSF problems. (2) Our method works particularly well in longer prediction settings. For instance, when the prediction length is 720, our approach improves the Informer’s MSE score by 21.63% for the Etth1 dataset and 20.00% for the traffic dataset, in contrast to the 10.00% and 14.96% improvements, respectively, for the prediction length of 24, and this trend is consistently observed across all different models and datasets. The improved performance with longer prediction settings makes sense, considering that the seasonal memory unit is highly effective at dealing with highly similar data, and our progressive training strategy effectively addresses the overfitting issues caused by increased prediction lengths. (3) Our method can further improve the performances of the SOTA LTSF model, FEDformer, on almost all tasks. Such experimental results prove that our method can be seamlessly plugged into varying Transformer-based LTSF systems even when these models are designed to explore the long dependencies and seasonal-trend features to improve the prediction capabilities. The frequency modules in FEDformer can be considered as another kind of memory-driven paradigm, and it is encouraging to observe that our methods bring out additional improvements.

D. Univariate Results

In Table IV, an extensive univariate results comparison is presented, comparing our method with various Transformer-based LTSF models. Notably, standout performers are indicated by values displayed in bold and red within each

Transformer-based LTSF model pair, as well as in contrast to the InParformer model. Since InParformer is not an open-source work, we directly listed the numbers from the original paper [12] for reference. The observations yield several important insights: (1) Our method consistently outperforms alternative Transformer-based models, including FEDformer and AutoFormer, across a spectrum of prediction lengths and datasets, especially in lengthier predictions. This is evidenced by reductions in both MSE and MAE. For instance, in the “Exchange” dataset with a prediction length of 720, our approach built upon FEDformer achieves an MSE of 1.126 compared to FEDformer’s 1.301, while InParformer records 1.172. (2) Our methodology demonstrates pronounced efficacy in extended prediction scenarios, yielding substantial performance gains relative to longer prediction lengths. This pattern is consistently observed across multiple models and datasets. For instance, on the “ETTh2” dataset with a prediction length of 720, our approach improves an MSE of 0.267 in comparison to FEDformer’s 0.278, and an MAE of 0.398 in comparison to AutoFormer’s 0.409, which also achieves competitive performances to InParformer. (3) The integration of our approach produces enhancements when embedded within the state-of-the-art LTSF model FEDformer and AutoFormer for univariate LTSF, thereby affirming its capability to augment performance in various Transformer-based systems designed to capture extended dependencies and seasonal-trend features. This incorporation leads to additional improvements, complementing existing mechanisms to capture intricate temporal patterns and long dependencies in these models. It is also encouraging to observe the compelling superiority of our proposed methodology in addressing univariate LTSF tasks across diverse contexts.

E. Ablation Study

The ablation study detailed in the Table.V examines the impact of various components of the proposed model on time series forecasting accuracy across three datasets: Etth1, Air Quality, and Traffic. This study specifically looks at

TABLE V: Ablation study for the decomposition of our approach, where p.t. is the progressive training scheme and mem refers to our memory approach (three repetitions).

datasets		Eth1				Air quality				Traffic			
prediction		24	48	168	336	24	48	168	336	24	48	168	336
Informer	MSE	0.550	0.644	1.110	1.237	0.562	0.692	0.833	0.852	0.381	0.440	0.567	0.572
	MAE	0.541	0.606	0.861	0.893	0.388	0.447	0.518	0.536	0.264	0.300	0.396	0.399
Informer + p.t.	MSE	0.510	0.651	1.021	1.136	0.583	0.690	0.813	0.848	0.377	0.431	0.564	0.571
	MAE	0.514	0.608	0.820	0.820	0.387	0.447	0.524	0.535	0.262	0.290	0.389	0.398
Informer + mem	MSE	0.510	0.588	1.009	1.161	0.569	0.680	0.769	0.794	0.331	0.352	0.411	0.417
	MAE	0.506	0.556	0.810	0.827	0.386	0.438	0.496	0.516	0.228	0.249	0.302	0.306
Informer + ours	MSE	0.495	0.582	0.981	1.098	0.542	0.650	0.720	0.773	0.324	0.351	0.405	0.397
	MAE	0.493	0.555	0.771	0.816	0.374	0.435	0.479	0.505	0.222	0.243	0.300	0.291
FedFormer	MSE	0.315	0.338	0.420	0.459	0.588	0.686	0.816	0.834	0.556	0.561	0.612	0.621
	MAE	0.381	0.392	0.443	0.465	0.412	0.457	0.515	0.518	0.364	0.359	0.381	0.383
FedFormer + p.t.	MSE	0.314	0.336	0.415	0.454	0.593	0.694	0.818	0.833	0.608	0.572	0.603	0.601
	MAE	0.377	0.383	0.440	0.459	0.412	0.459	0.513	0.518	0.392	0.366	0.378	0.374
FedFormer + mem	MSE	0.308	0.336	0.411	0.450	0.590	0.689	0.812	0.830	0.575	0.567	0.601	0.590
	MAE	0.372	0.385	0.446	0.461	0.414	0.457	0.509	0.515	0.374	0.362	0.368	0.359
FedFormer + ours	MSE	0.304	0.335	0.407	0.451	0.590	0.694	0.805	0.827	0.611	0.588	0.587	0.584
	MAE	0.370	0.381	0.438	0.454	0.411	0.459	0.504	0.515	0.412	0.373	0.364	0.350

TABLE VI: Ablation study of different memory matrix initialization methods (three repetitions).

datasets		Eth1				Eth2				Weather			
prediction		24	48	336	720	24	48	168	336	24	48	168	336
Informer+mem (ours)	MSE	0.510	0.588	1.009	1.161	0.553	1.204	5.069	4.883	0.243	0.350	0.519	0.556
	MAE	0.506	0.556	0.810	0.843	0.578	0.879	2.043	1.869	0.328	0.411	0.525	0.544
Informer+mem (Identity matrix)	MSE	0.537	0.571	1.168	1.224	0.592	1.242	6.454	5.034	0.254	0.353	0.521	0.567
	MAE	0.528	0.546	0.848	0.894	0.602	0.888	2.251	1.943	0.335	0.412	0.530	0.549
FedFormer+mem (ours)	MSE	0.308	0.336	0.454	0.476	0.222	0.280	0.409	0.488	0.153	0.194	0.268	0.311
	MAE	0.377	0.383	0.459	0.463	0.314	0.381	0.416	0.471	0.239	0.280	0.332	0.365
FedFormer+mem (Identity matrix)	MSE	0.310	0.352	0.467	0.488	0.218	0.283	0.417	0.503	0.167	0.211	0.276	0.325
	MAE	0.383	0.394	0.471	0.480	0.318	0.390	0.422	0.484	0.246	0.292	0.357	0.381

the performance of the Informer and FedFormer model and their enhancements through progressive training (p.t.), our memory approach (mem), and a combination of both referred to as “ours.” From the results, we can draw several key observations. Both the progressive training strategy and the memory approach independently improve the Informer’s forecasting accuracy. For instance, in the Eth1 dataset, applying progressive training reduced the MSE from 1.110 to 1.021 for a 168-hour prediction horizon, and incorporating the memory approach further reduced it to 1.009. Similar improvements are seen in MAE metrics and across other datasets. The combination of progressive training and the memory approach under “Informer + ours” consistently yields the best results. For example, it achieves the lowest MSE of 0.495 and MAE of 0.493 for a 24-step forecast on the Eth1 dataset. This pattern holds across all datasets and prediction horizons, indicating a synergistic effect when both enhancements are applied together. The improvements are more pronounced for longer prediction horizons. For instance, in the Traffic dataset, the “Informer + ours” configuration reduces the MSE to 0.405 and the MAE to 0.300 for a 168-step forecast, suggesting that the proposed components are particularly effective at addressing challenges in long-term sequence forecasting (LTSF). While the Informer model and its enhancements focus on incremental

improvements, the FedFormer model, both alone and with added enhancements (progressive training, memory approach, and combined), shows varied performance across datasets. “FedFormer+ours” achieves better MSE and MAE scores in the shorter and longer prediction horizons for the Eth1 dataset, and always outperforms the base model, especially in the Air Quality and Traffic datasets for longer horizons. These detailed observations confirm the effectiveness of the combined approach in improving forecasting accuracy, especially in longer prediction horizons. This suggests that the integration of these components can effectively tackle the inherent challenges in LTSF problems, making it a valuable strategy for enhancing time series forecasting models.

Table VI presents the findings from our second ablation study focused on evaluating the efficacy of different memory matrix initialization methods within our proposed model across three distinct datasets: Eth1, Eth2, and Weather. This study specifically compares the performance of our model using a seasonal memory matrix (denoted as “ours”) against a baseline initialization approach employing an Identity matrix [45], [46]. The results delineated in the table underscore the superior performance of the Informer model augmented with our seasonal memory matrix across the majority of tasks and horizons, particularly highlighting its robustness

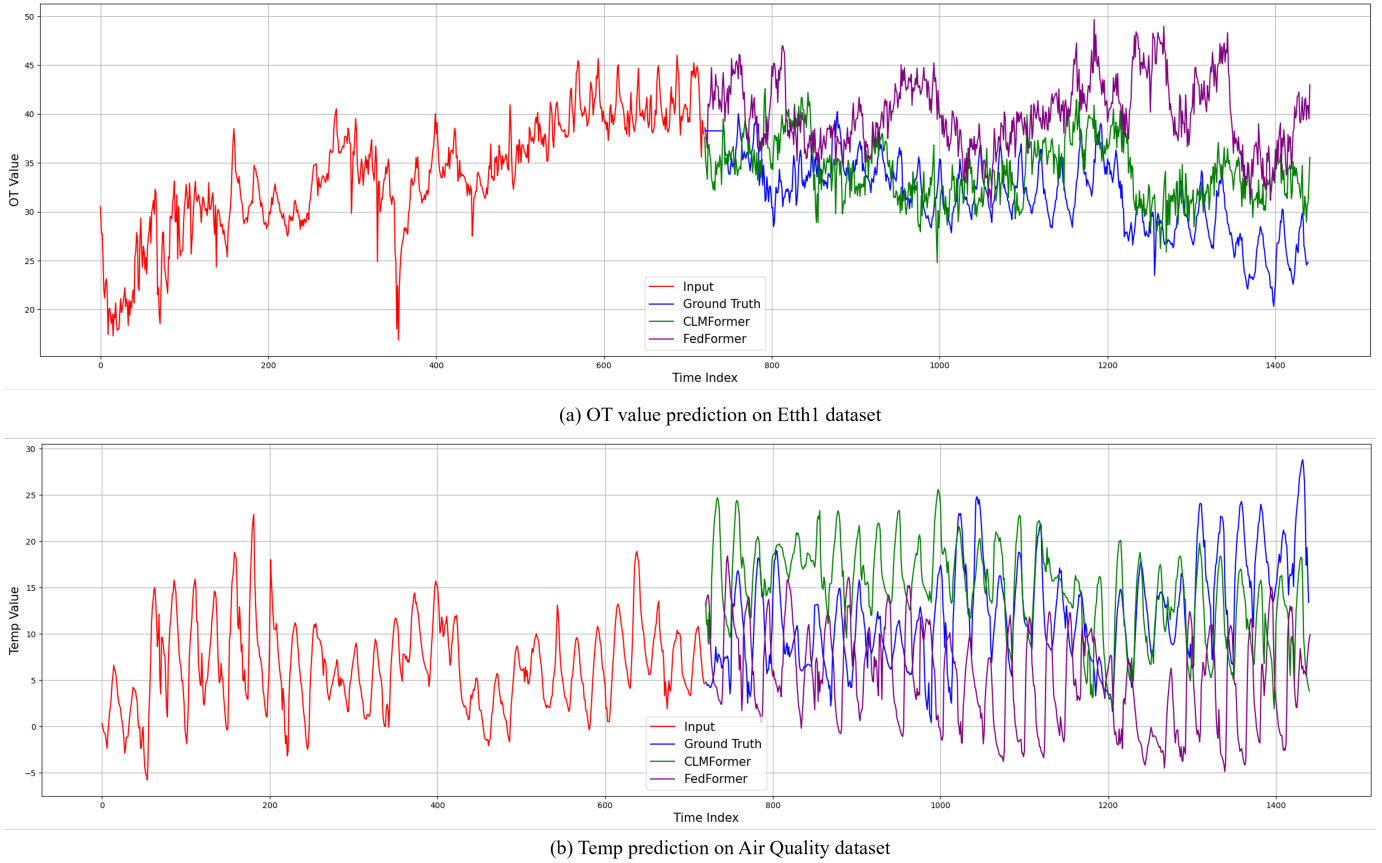


Fig. 4: Samples of time series data from the ETTh1 and Air Quality datasets, along with predictions by FedFormer and our CLMFormer. We employ multivariate settings with prediction lengths of 720 and visualize the OT value and temperature value for the ETTh1 and Air Quality datasets, respectively.

in capturing long-term dependencies and complex temporal dynamics inherent in the datasets. For instance, in the ETTh1 dataset, our approach consistently outperforms the Identity matrix initialization in both MSE and MAE metrics across all forecasting horizons, with significant improvements observed at longer horizons (336 and 720 predictions), which underscores the enhanced capacity of our model to retain and leverage long-term historical information for accurate future predictions. Moreover, the study also explores the efficacy of these memory matrix initialization methods within the FedFormer model, further substantiating the adaptability and effectiveness of our seasonal memory matrix in enhancing forecasting performance. Notably, the FedFormer model with our memory matrix initialization demonstrates remarkable improvements over the Identity matrix, especially in the ETTh2 and Weather datasets, indicating the generalizability of our proposed method across different models and datasets. This ablation study clearly demonstrates that our seasonal memory matrix significantly outperforms the traditional Identity matrix in capturing long-term dependencies and intricate temporal patterns within time series data. By providing a more sophisticated mechanism for initializing the memory matrix, our approach enables the model to better understand and predict future values based on historical data, thereby setting a new benchmark for performance in time series forecasting tasks.

This validation not only reinforces the value of our adaptations to the memory matrix but also highlights the potential for further innovations in enhancing the capabilities of time series forecasting models.

F. Case Study

In this section, we embark on two case studies to conduct a qualitative evaluation of the predictive capabilities of our CLMFormer and FedFormer. Specifically, we present the input and ground truth instances with the predictions rendered by both FedFormer and CLMFormer over a forecast length of 720 intervals within the ETTh1 and Air Quality datasets, as depicted in Figure 4. Across both subplots, it is discernible that the predictions generated by our CLMFormer, represented in green, more closely adhere to the ground truth, delineated in blue, exhibiting similar trends in contrast to those of FedFormer. This convergence with the ground truth underscores the enhanced capability of CLMFormer to generate both extensive and high-fidelity predictions. Moreover, it becomes evident that the FedFormer’s predictions, illustrated in purple, tend to perpetuate the trends observed in the input data, adhering to a linear trajectory. In contrast, CLMFormer is adept at capturing non-linear relationships. We postulate that this is attributable to our proposed seasonal memory-driven forecasting modules, which empower the model to internalize

seasonal patterns from the entire corpus of training data, thereby furnishing more accurate and elongated predictive insights.

V. CONCLUSION

In this paper, we propose a novel pipeline, named CLMFormer, to revitalize Transformer-based LTSF systems by mitigating data redundancy stemming from the rolling forecasting settings. We first discuss the influence of rolling forecasting settings on Transformer-based LTSF systems. Subsequently, we train a seasonal memory-driven Transformer-based model in a progressive fashion. We demonstrate that seasonal memory improves the model’s ability to comprehend both multivariate and univariate sequential patterns from highly similar training samples. In addition, the progressive training schedule can effectively address overfitting issues in LTSF. We validate our methods on six public real-life benchmarks with five different prediction lengths ranging from 24 to 720 time steps. The results show that our method works exceptionally well with longer prediction sequences and can be seamlessly integrated into varying Transformer-based LTSF models and achieve up to 30% improvement.

ACKNOWLEDGEMENTS

This work was supported by the Australian Research Council Discovery Project No. 210101347 and the Australian Research Council (ARC) Discovery Early Career Researcher Award (DECRA) under grant No. DE190100626.

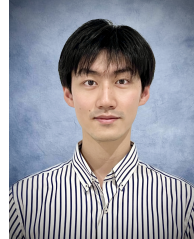
REFERENCES

- [1] Y. Tang, Z. Song, Y. Zhu, H. Yuan, M. Hou, J. Ji, C. Tang, and J. Li, “A survey on machine learning models for financial time series forecasting,” *Neurocomputing*, vol. 512, pp. 363–380, 2022.
- [2] K. Bi, L. Xie, H. Zhang, X. Chen, X. Gu, and Q. Tian, “Accurate medium-range global weather forecasting with 3d neural networks,” *Nature*, pp. 1–6, 2023.
- [3] G. Raman, B. Ashraf, Y. K. Demir, C. D. Kershaw, S. Cheruku, M. Atis, A. Atis, M. Atar, W. Chen, I. Ibrahim, T. Bat, and M. Mete, “Machine learning prediction for COVID-19 disease severity at hospital admission,” *BMC Medical Informatics Decis. Mak.*, vol. 23, no. 1, p. 46, 2023.
- [4] A. Vaswani, N. Shazeer, N. Parmar, J. Uszkoreit, L. Jones, A. N. Gomez, E. Kaiser, and I. Polosukhin, “Attention is all you need,” in *NeurIPS*, 2017.
- [5] M. Li, P.-Y. Huang, X. Chang, J. Hu, Y. Yang, and A. Hauptmann, “Video pivoting unsupervised multi-modal machine translation,” *IEEE Transactions on Pattern Analysis and Machine Intelligence*, 2022.
- [6] X. Lin, S. Sun, W. Huang, B. Sheng, P. Li, and D. D. Feng, “Eapt: efficient attention pyramid transformer for image processing,” *IEEE Transactions on Multimedia*, 2021.
- [7] A. Yang, S. Lin, C.-H. Yeh, M. Shu, Y. Yang, and X. Chang, “Context matters: Distilling knowledge graph for enhanced object detection,” *IEEE Transactions on Multimedia*, 2023.
- [8] J. Liu, W. Wang, S. Chen, X. Zhu, and J. Liu, “Sounding video generator: A unified framework for text-guided sounding video generation,” *IEEE Transactions on Multimedia*, 2023.
- [9] Y. Su, J. Deng, R. Sun, G. Lin, H. Su, and Q. Wu, “A unified transformer framework for group-based segmentation: Co-segmentation, co-saliency detection and video salient object detection,” *IEEE Transactions on Multimedia*, 2023.
- [10] M. Li, B. Lin, Z. Chen, H. Lin, X. Liang, and X. Chang, “Dynamic graph enhanced contrastive learning for chest x-ray report generation,” *arXiv preprint arXiv:2303.10323*, 2023.
- [11] M. Li, R. Liu, F. Wang, X. Chang, and X. Liang, “Auxiliary signal-guided knowledge encoder-decoder for medical report generation,” *World Wide Web*, vol. 26, no. 1, pp. 253–270, 2023.
- [12] H. Cao, Z. Huang, T. Yao, J. Wang, H. He, and Y. Wang, “Inparformer: Evolutionary decomposition transformers with interactive parallel attention for long-term time series forecasting,” in *Proceedings of the AAAI Conference on Artificial Intelligence*, vol. 37, no. 6, 2023, pp. 6906–6915.
- [13] Y. Nie, N. H. Nguyen, P. Sinthong, and J. Kalagnanam, “A time series is worth 64 words: Long-term forecasting with transformers,” in *The Eleventh International Conference on Learning Representations, ICLR 2023, Kigali, Rwanda, May 1-5, 2023*. OpenReview.net, 2023. [Online]. Available: <https://openreview.net/pdf?id=Jbdc0vTOcol>
- [14] T. Zhou, Z. Ma, Q. Wen, X. Wang, L. Sun, and R. Jin, “Fedformer: Frequency enhanced decomposed transformer for long-term series forecasting,” in *International Conference on Machine Learning*. PMLR, 2022, pp. 27 268–27 286.
- [15] H. Zhou, S. Zhang, J. Peng, S. Zhang, J. Li, H. Xiong, and W. Zhang, “Informer: Beyond efficient transformer for long sequence time-series forecasting,” in *AAAI*, 2021.
- [16] S. Hochreiter and J. Schmidhuber, “Long short-term memory,” *Neural Computation*, vol. 9, pp. 1735–1780, 1997.
- [17] Y. Qin, D. Song, H. Chen, W. Cheng, G. Jiang, and G. W. Cottrell, “A dual-stage attention-based recurrent neural network for time series prediction,” in *IJCAI*, 2017.
- [18] R. Wen, K. Torkkola, B. Narayanaswamy, and D. Madeka, “A multi-horizon quantile recurrent forecaster,” *arXiv:1711.11053*, 2018.
- [19] H. Wu, J. Xu, J. Wang, and M. Long, “Autoformer: Decomposition transformers with auto-correlation for long-term series forecasting,” *Advances in Neural Information Processing Systems*, vol. 34, pp. 22 419–22 430, 2021.
- [20] J. Wang, S. Qian, J. Hu, and R. Hong, “Positive unlabeled fake news detection via multi-modal masked transformer network,” *IEEE Transactions on Multimedia*, 2023.
- [21] Y. Du, M. Wang, W. Zhou, and H. Li, “Progressive similarity preservation learning for deep scalable product quantization,” *IEEE Transactions on Multimedia*, 2023.
- [22] J. Pan, S. Yang, L. G. Foo, Q. Ke, H. Rahmani, Z. Fan, and J. Liu, “Progressive channel-shrinking network,” *IEEE Transactions on Multimedia*, 2023.
- [23] K. Benidis, S. S. Rangapuram, V. Flunkert, Y. Wang, D. C. Maddix, A. C. Türkmen, J. Gasthaus, M. Bohlke-Schneider, D. Salinas, L. Stella, F. Aubet, L. Callot, and T. Januschowski, “Deep learning for time series forecasting: Tutorial and literature survey,” *ACM Comput. Surv.*, vol. 55, no. 6, pp. 121:1–121:36, 2023.
- [24] G. E. Box and G. M. Jenkins, “Some recent advances in forecasting and control,” *Journal of the Royal Statistical Society. Series C (Applied Statistics)*, vol. 17, no. 2, pp. 91–109, 1968.
- [25] E. S. Gardner Jr, “Exponential smoothing: The state of the art,” *Journal of forecasting*, vol. 4, no. 1, pp. 1–28, 1985.
- [26] R. B. Cleveland, W. S. Cleveland, J. E. McRae, and I. Terpenning, “Stl: A seasonal-trend decomposition,” *J. Off. Stat.*, vol. 6, no. 1, pp. 3–73, 1990.
- [27] K. Cho, B. Van Merriënboer, D. Bahdanau, and Y. Bengio, “On the properties of neural machine translation: Encoder-decoder approaches,” *arXiv preprint arXiv:1409.1259*, 2014.
- [28] D. Salinas, V. Flunkert, J. Gasthaus, and T. Januschowski, “Deepar: Probabilistic forecasting with autoregressive recurrent networks,” *International Journal of Forecasting*, vol. 36, no. 3, pp. 1181–1191, 2020.
- [29] S. Bengio, O. Vinyals, N. Jaitly, and N. Shazeer, “Scheduled sampling for sequence prediction with recurrent neural networks,” *Advances in neural information processing systems*, vol. 28, 2015.
- [30] Q. Wen, T. Zhou, C. Zhang, W. Chen, Z. Ma, J. Yan, and L. Sun, “Transformers in time series: A survey,” *arXiv preprint arXiv:2202.07125*, 2022.
- [31] M. Jin, G. Shi, Y.-F. Li, Q. Wen, B. Xiong, T. Zhou, and S. Pan, “How expressive are spectral-temporal graph neural networks for time series forecasting?” *arXiv preprint arXiv:2305.06587*, 2023.
- [32] S. Wu, X. Xiao, Q. Ding, P. Zhao, Y. Wei, and J. Huang, “Adversarial sparse transformer for time series forecasting,” in *NeurIPS*, 2020.
- [33] A. Zeng, M. Chen, L. Zhang, and Q. Xu, “Are transformers effective for time series forecasting?” in *Proceedings of the AAAI conference on artificial intelligence*, vol. 37, no. 9, 2023, pp. 11 121–11 128.
- [34] J. Devlin, M.-W. Chang, K. Lee, and K. Toutanova, “Bert: Pre-training of deep bidirectional transformers for language understanding,” in *NAACL*, 2018.
- [35] C. M. Bishop, “Training with noise is equivalent to tikhonov regularization,” *Neural Computation*, vol. 7, pp. 108–116, 1995.
- [36] S. Wager, S. I. Wang, and P. Liang, “Dropout training as adaptive regularization,” in *NeurIPS*, 2013.

- [37] S. Zhai and Z. Zhang, "Dropout training of matrix factorization and autoencoder for link prediction in sparse graphs," in *SDM*, 2015.
- [38] P. Morerio, J. Cavazza, R. Volpi, R. Vidal, and V. Murino, "Curriculum dropout," in *ICCV*, 2017.
- [39] C. Ma, C. Shen, A. R. Dick, Q. Wu, P. Wang, A. van den Hengel, and I. D. Reid, "Visual question answering with memory-augmented networks," in *CVPR*, 2018.
- [40] C. Ma, L. Ma, Y. Zhang, J. Sun, X. Liu, and M. Coates, "Memory augmented graph neural networks for sequential recommendation," in *AAAI*, 2020.
- [41] Z. Fei, "Memory-augmented image captioning," in *AAAI*, 2021.
- [42] D. Xu, W. Cheng, B. Zong, D. Song, J. Ni, W. Yu, Y. Liu, H. Chen, and X. Zhang, "Tensorized lstm with adaptive shared memory for learning trends in multivariate time series," in *AAAI*, 2020.
- [43] M. Jiang, J. Wu, X. Shi, and M. Zhang, "Transformer based memory network for sentiment analysis of web comments," *IEEE Access*, vol. 7, pp. 179 942–179 953, 2019.
- [44] A. Banino, A. P. Badia, R. Köster, M. J. Chadwick, V. F. Zambaldi, D. Hassabis, C. Barry, M. Botvinick, D. Kumaran, and C. Blundell, "MEMO: A deep network for flexible combination of episodic memories," in *ICLR*, 2020.
- [45] Z. Chen, Y. Song, T.-H. Chang, and X. Wan, "Generating radiology reports via memory-driven transformer," in *EMNLP*, 2020.
- [46] X. Ma, Y. Wang, M. J. Dousti, P. Koehn, and J. Pino, "Streaming simultaneous speech translation with augmented memory transformer," in *ICASSP*, 2021.
- [47] T. Zhou, Z. Ma, X. Wang, Q. Wen, L. Sun, T. Yao, W. Yin, and R. Jin, "Film: Frequency improved legendre memory model for long-term time series forecasting," in *NeurIPS*, 2022.



Mingfei Han is currently pursuing the Ph.D. degree under the supervision of Prof. Xiaojun Chang with University of Technology Sydney. He received the B.Eng. degree from Nankai University and the M.Eng. degree from the University of Chinese Academy of Sciences. His research interests lie in computer vision and machine learning, with a particular emphasis on large vision-language models and video object perception.



Changlin Li is a Postdoctoral Researcher in ReLER Lab, Australian Artificial Intelligence Institute, University of Technology Sydney (UTS). He received his Ph.D. degree from UTS in 2023. Prior to his Ph.D. study, he received his B.E. degree in Computer Science in 2019, from University of Science and Technology of China. He currently serves as a reviewer of CVPR, ICCV, ECCV, ICML, NeurIPS, T-PAMI, T-IP, etc. His main research ambition is to explore more efficient and more intelligent neural network architectures. He is also interested in computer vision tasks such as activity recognition and has won first place in the TRECVID ActEV 2019 grand challenge.



Lina Yao (Senior Member, IEEE) is a senior principal research scientist and a Science Lead for Translational Machine Learning @ CSIRO's Data61. Her current research interests include data mining and machine learning with applications to Internet of Things, information filtering and recommending, human activity recognition, and brain-computer interface.



Mingjie Li is a post-doctoral researcher at Stanford University. His research interests include machine learning and computer vision, especially on the topic of medical image understanding and medical report generation. Before joining Stanford, he received his Ph.D. degree from UTS and his master degree from Shanghai Jiao Tong University.



Rui Liu is currently pursuing her Ph.D. degree under the supervision of Prof. Xiaojun Chang at the University of Technology Sydney and is a research assistant at Monash Children's Hospital. Her research interests include machine learning and artificial intelligence in public health, especially in medical image analysis. Before joining UTS, she received her master's degree from Monash University with First Class Honors.



Xiaojun Chang is a Professor at Australian Artificial Intelligence Institute, University of Technology Sydney. He is also an Honorary Professor at the School of Computing Technologies, RMIT University. Before joining UTS, he was an Associate Professor at the School of Computing Technologies, RMIT University, Australia. After graduation, he subsequently worked as a Postdoc Research Fellow at School of Computer Science, Carnegie Mellon University, Lecturer and Senior Lecturer in the Faculty of Information Technology, Monash University, Australia. He has spent most of his time working on exploring multiple signals (visual, acoustic, textual) for automatic content analysis in unconstrained or surveillance videos. He has achieved top performances in various international competitions, such as TRECVID MED, TRECVID SIN, and TRECVID AVS.



Guangsi Shi received a M.Eng from University of Science and Technology Beijing(USTB), Beijing, China, in 2017. He is currently pursuing his Ph.D. degree at Monash University, Melbourne, Australia. His research focuses on Knowledge-based Machine Intelligence, Machine & Deep Graph Learning, AI for Science & Engineering, and Robotics.



Ling Chen is a Professor with the Australian Artificial Intelligence Institute, University of Technology Sydney. She received PhD from Nanyang Technological University, Singapore. Her research area is machine learning and data mining. Her recent research focuses on anomaly detection from complex structured data, hashing and representation learning for various types of data, and reinforcement learning in text-based interactive systems. Her papers appear in major journals and conferences including IEEE TPAMI, IEEE TNNLS, NeurIPS and IJCAI. She is an editorial member of the Elsevier Journal of Data and Knowledge Engineering, the Springer Journal of Data Science and Analytics, and the IEEE Journal of Social Computing.